STATIC-VIBRATIONAL DESIGN OF A BONNET WITH FRAME TOPOLOGICAL OPTIMIZATION

D. Col[1], F. Furini[2], O. Mueller[3], R. Trivero[4]

Abstract

This paper presents an analytical-experimental methodology in the design and optimisation process of a bonnet for a prototype roadster car named Argento Vivo and built by Pininfarina in co-operation with Honda. A part of this work has been carried out within the European Project HIPOP(High Performance Optimisation).

The finite element model has been realised by using the pre-processor MSC/PATRAN with CAD PTC direct interface. At the beginning the bonnet analytical model has been validated by comparing the torsional stiffness calculation by MSC/NASTRAN Solution 101 with the results obtained by Pininfarina Testing Laboratory. Then an analytical modal analysis has been carried out by SOLUTION 103 of MSC/NASTRAN with the frequency and modal shape definition. Then by a pre-test analysis, i.e. by the identification of a reduced analytical model formed by a number of nodes very lower than the complete analytical mode, but able to completely approximate the dynamic behaviour, by using the MAC as control index, a modal experimental analysis has been carried out on the bonnet on the reduced set of points. A considerable importance is given to the methodologies by which the modal parameters are drawn by the frequency response functions (FRF) experimentally obtained by the software LMS Cada-X.

At the end a bonnet frame topological optimisation has been carried out by MSC/CONSTRUCT that, with the structure stress behaviour known, acts directly on the material distribution by adding or removing the material in those points on which the stresses reach more or less high values, by creating holes and opening in the area to be optimised, by maintaining the torsional and/or bending stiffness values within the requirements. In this way it is possible to obtain a mass reduction, and therefore cost reduction without jeopardising the static characteristics, or if this occurs, the variations are within defined values. A further model verification for the optimised design has been carried out. This type of applications is perfect for the automotive sector where the structural optimisation, in order to act on the vehicle stiffness with advantages both in terms of stability, safety, comfort and costs is needed almost everyday.

The aim is the presentation of a static-vibrational analysis methodology for the bonnet design for a car realised by Pininfarina, named Argento Vivo, built as a prototype and identified as a two-seats roadster car with a complete hidden hard top (Fig.1).

The frame is made by aluminium alloy extrusions for a total weight of 87 Kg. The bonnet is made of steel and formed by an outer skin, a bonded lower frame and some reinforcements applied in line with the anchorage points with the frame.

The aim of this frame is to stiffen the structure, very flexible, due to its considerable dimensions and its particular shape. The bonnet metal sheet thickness is 0.8 mm.

1. Industrie Pininfarina, Via Lesna 78-80, 10095 Grugliasco (Torino) Italy
2. Industrie Pininfarina, Via Lesna 78-80, 10095 Grugliasco (Torino) Italy
3. University of Karlsruhe – Institute of Machine Design, Kaiserstrasse 12, 76131 Karlsruhe - Germany
4. Industrie Pininfarina, Via Lesna 78-80, 10095 Grugliasco (Torino) Italy

Figure 1: Argento Vivo

1. Finite element analytical model and torsional analysis

Using the direct interface of CAD model made by ProEngineer with the pre-post processor MSC/PATRAN has carried out the bonnet mesh. The finite element model obtained is characterised by 58369 nodes, 54564 elements CQUAD and 4285 elements CTRIA3.
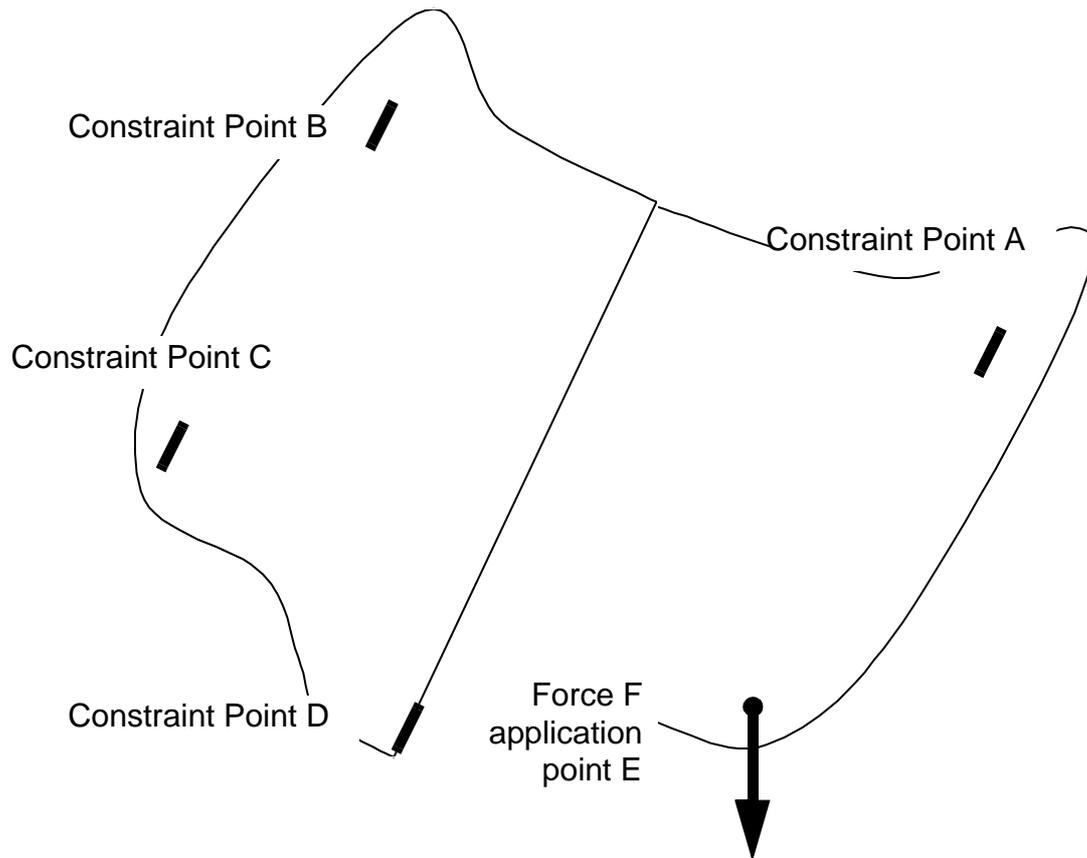
Figure 2: Loads and constraints

The percentage of 3 nodes triangular elements in the model is about of 5% with respect to the quantity of 4 node elements. Figure 2 shows in particular that points A and B are rigid joints with all the six degrees of freedom blocked, while point D has the translations blocked and the rotations free. This constraint simulates the ball joint used to carry out the experimental test. The force applied to point E has a 100 N value and is downward. The original mathematical model has given a 32.89 N/mm (199.7 Nm/Deg) torsional stiffness value corresponding to a 5.15 mrad torsional angle and a 3.04 mm displacement in the point where experimentally measured. Fig. 3 shows the bonnet finite element model under load with the force application and constraint points viewed from the bottom. Fig. 4 shows the bonnet deformed "shade" model subjected to torsion, while Fig. 5 shows respectively the local displacement behaviour in z (mm) and the stress behaviour (N/mm^2), calculated by using Von Mises cracking assumption.

2.   Torsional stiffness experimental measurement

This procedure is applied to the bonnet, but is applicable to other similar car parts too, like the trunk lid. The equipment used is the following:
   - Retaining fixture
   - Pillar with adjustable supports
   - 300 N capacity load cell
   - X and y linear motion recorder
   - Motion amplifiers (at least two)
   - Linear motion transducer (cable transducer) with 200 mm capacity at least
   - C clamps or equivalent blocking system
   - Force meter with notch and hook attachment

This equipment should be suitably adjusted.

Retaining procedure (Fig. 6)
   1.   Secure the bonnet to the retaining fixture by bolts fixing it to the hinged rigid crossmember.
   2.   Slacken the adjustable retainers on the fixing equipment in order to allow to the rigid brackets to rotate.
   3.   Position the pillar in one of the bonnet front angles and adjust it until it is in the horizontal position. The pillar support should be positioned at 25 mm from the bonnet lower edge.
   4.   Secure the C clamp (or the equivalent equipment) in the bonnet front angle; opposite to the proceeding one and not supported at 25 mm from the bonnet lower edge.
   5.   Position the linear motion transducer below the angle not supported by the bonnet and connect the transducer cable to the C clamp.
   6.   Adjust the load cell in order to record a 300 N max load.
   7.   Adjust the transducer in order to read on the recorder a 200 mm-max displacement.
   8.   The load should be directly applied to the C clamp (or equivalent system) thread in order to be closer to the more external section of bonnet.
   9.   Apply a 50, 100 e 180 N vertical load to the bonnet downward according the above-mentioned methodology.
   10.   Record the load/deformation run and the hysteresis curve.
   11.   Replace, on the force meters, the notch attachment with the hook one.
   12.   Repeat points 9 and 10, but applying a 50,100 and 180 N vertical load to the bonnet upward. Slowly release the load (also in this case the 180 N load application involve the subsequent bonnet scrapping).
   13.   Measure and record the distance between support and load application point. This measure is required to calculate the torsional stiffness.
   14.   The torsion results are calculated as follows:

$$Torsional\ stiffness = \frac{(Force)\cdot(Distance\ between\ support\ and\ load\ application\ po\operatorname{int})}{Bonnet\ angular\ displacement}\left[\frac{N\cdot m}{DEG}\right]$$

with

$$Bonnet\ angular\ displacement = Arctan\left(\frac{Bonnet\ corner\ vertical\ displacement}{Distance\ between\ support\ and\ load\ application\ po\operatorname{int}}\right)$$

or

$$Torsional\ stiffness = \frac{Force}{Bonnet\ corner\ vertical\ displacement} \quad \left[\frac{N}{mm}\right]$$

The torsion test is carried out also by a centre retainer when the bonnet is equipped with a centre lock; in this case all is carried out like in the preceding test with the exception of the type of retainer. In fact for the centre retaining point it is used a ball joint in order to allow to the bonnet to rotate with respect to the point, but not to translate. Following the above mentioned procedures it is possible to obtain the temporary displacement, permanent displacement and stiffness values according to the constraint and load modes. These results are visible on Table 1 here below. The stiffness values meet the requirements

Load [N]	Temp. Displ. [mm]	Perm. Displ. [mm]	Stiffness [N/mm]	
UPWARD LOAD **LOAD WITH CENTRE RETAINER**				
			Required value	Measured value
100	**2.9**	**0.2**	**≥20**	**34.48**
DOWNWARD LOAD				
LOAD WITH CENTRE RETAINER				
Load [N]	Temp. Displ. [mm]	Perm. Displ. [mm]	Stiffness [N/mm]	
			Required value	Measured value
100	**3.3**	**0.1**	**≥20**	**30.30**

Tab. 1 Displacement and stiffness values with upward and downward load

3. Modal analysis

Usually the first step to be carried out in the dynamic analysis is the definition of frequencies and modal shapes of the structure not dumped. These results define the structure natural behaviour if subjected to a dynamic load; therefore it is possible to obtain the structure natural frequencies, i.e. the frequencies at which the structure tends to vibrate if subjected to an external stress. Each resonance frequency is assigned to a defined modal shape.

The resonance frequencies and the modal shapes are lied to the type of structure and the constraint conditions. By changing the structural characteristics, the structure frequency changes, while the modal shape could remain the same. The calculation of structure frequencies and the relating modal shapes is made by solving a problem at eigenvalues that represent the frequencies, while the eigenvectors represent the modal shapes.

After the static stiffness calculation the eigenvalues and the relating eigenvectors have been calculated for the modal analysis. It is to be noted that the problem has a considerable dimension as the matrix used to obtain the eigenvalues and the eigenvectors have these dimensions *(58369 · 6d.o.f.)x(58369 · 6d.o.f.)*. The dynamic matrix of the problem would be considerable and the problem of eigenvalues and eigenvectors would be very difficult.

Among the different available methods it has been used Lanczos' method. Table 2 shows the analytical frequencies concerning the first six modes.

Mode	Analytical frequency (Hz)	Mode description
1	17.313	Bending plane zy
2	19.202	Stiffening frame bending
3	21.405	First torsional
4	23.171	Second torsional
5	33.112	Bending plane xy
6	37.991	Bending plane zx

Table 2 Analytical model frequencies and modal shapes

4. Pre-test analysis

In order to carry out the correlation between analytical and experimental model, it should be identified on the finite element model represented by 58369, nodes those nodes that would approximate at best the measuring points that should be identified and measured. This is useful to obtain a reduced analytical model corresponding to the scheme that will be used for the experimental tests. This reduced model is a finite element model having as nodes as the measuring points on which the structure mass is distributed and that are considered as "master" degrees of freedom. The remaining degrees of freedom with mass equal to zero, but lied by stiffness elements are considered as degrees of freedom "slave". Therefore it is needed a Guyan's reduction to obtain the mass and stiffness matrix concerning the reduced model by moving the problem having dimensions *(58369 · 6d.o.f.)x(58369 · 6d.o.f.)* to the following *(164 · 6d.o.f.)x(164 · 6d.o.f.)*, obviously more simplified where the points used to experimentally measure the bonnet are 164.

The eigenvalues and the eigenvectors are obtained by the reduced model and then the MAC index is calculated among the reduced model eigenvectors (by considering only the master degrees of freedom) and the initial complete model ones (by considering only the elements corresponding to the reduced model master degrees)

$$MAC(p,x) = \frac{\left(\left\{\Phi_{rid}\right\}_p^T \left\{\Phi_{com}\right\}_x^*\right)^2}{\left(\left\{\Phi_{rid}^T\right\}_p \left\{\Phi_{rid}\right\}_p^*\right)\left(\left\{\Phi_{com}^T\right\}_x \left\{\Phi_{com}\right\}_x^*\right)}$$

$\left(\Phi_{rid}\right)_p$ is the p-nth eigenvector of the reduced analytical model.

$\left(\Phi_{com}\right)_x$ is the x-nth eigenvector of the complete analytical model.

The asterisk used as index of self-vectors suggests to consider the complex joined eigenvector. This index means that a MAC value equal to 1 indicates a perfect correlation among the modes of complete model and those of the reduced one, even if usually a value higher than 0,9 already indicates a good correlation, while a low index means a bad correlation. [2]

The resulting matrix is shown on Fig. 7 where from the unit values of the elements on the main diagonal and from the values practically equal to zero of the elements out of the diagonal it is possible to understand that the modal shapes are equal, giving a positive result of the pre-test analysis. It follows that the reduced model represents very well the complete one and that in practice the elements of reduced one eigenvectors result like obtained by the complete model eigenvectors; this confirm the validity of the points chosen to carry out the experimental measurements.
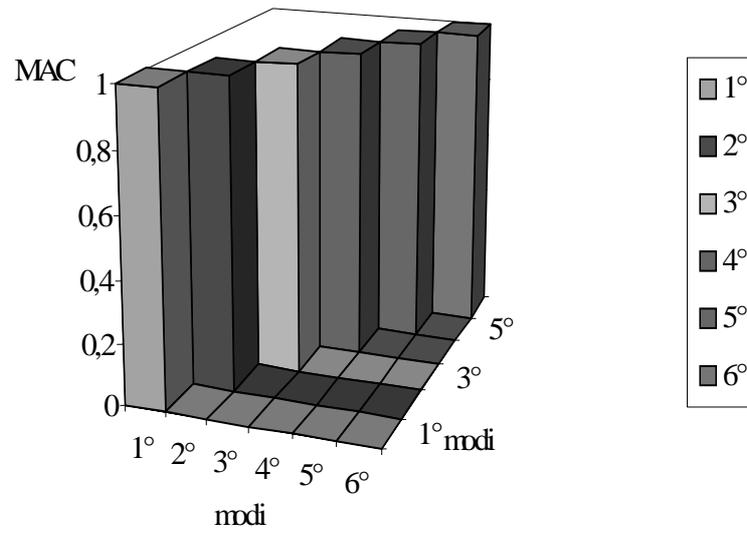
Figure 7: Pre-test analysis: MAC between complete and reduced model

5. Equipment used for the experimental measurement

To acquire and to process the data, the following equipment has been used:
- No. 2 power amplifiers LDS, PA 1000L & PA 500L, for feeding and checking the electromagnetic shakers;
- No. 2 electromagnetic dynamic shakers LDS, V455 (489 N) & V406 (196 N);
- No. 2 force transducers (load cells) PCB;
- No. 12 monoaxial accelerometers PCB 336C04 FLEXCELL;
- Glue (Loctite) to secure the plates to the bonnet;
- Rack to raise the bonnet equipped with elastic hooks;
- Equipment measuring the accelerometer signals and generating random and sinusoidal signals (Workstation HP 715/100 interfaced with DIFA SCADAS II, 20 input channels and 4 output QDAC, software LMS) ;
- Data processor with sofware dedicated to the modal analysis and to generate random and sinusoidal signals (software LMS module Advanced Modal Analysis).

6. Bonnet constraint conditions and experimental set up

To characterise the dynamic behaviour also in the perspective of a dynamic optimisation we will refer to a free-free constraint condition. For this purpose very low stiffness suspensions are needed. The structure should have rigid modes, due to the suspensions as low as to avoid dynamic interference. A good approach is to have the highest rigid mode frequency that is one tenth lower than that corresponding to the first flexible mode of the structure under analysis. The most used suspensions are elastics. The elastics have been hooked to the bonnet by using two screws on the same in particularly rigid areas, while their opposite ends have been connected by small manual movable hoists to two portals. These are dynamically insulated from the floor by rubber bases in order to avoid any vibrations, deriving from the surrounding systems, to the bonnet. The experimental set up is shown on Fig. 8.

The workstation HP 715/100 manages the measuring operation by operator's direct check and by a dedicated software LMS-Cada-X. To this unit, by a SCSI cable, is connected the system DIFA SCADAS II that controls the two electromagnetic shakers amplifiers. The acquisition unit receives the signals deriving from the two load cells and the 12 accelerometers.

The workstation, interfaced with the acquisition unit by software control, sends the shaker signals to the amplifiers and then to the shakers. By the load cells it is possible to measure the load applied to the bonnet and to send it to the acquisition unit and then to the workstation where is processed by the software to be used with the signals deriving from the accelerometers to obtain the FRF.

Each measurement is based on the record of accelerations in 12 points by the same number of monoaxial accelerometers. The accelerometers originate electrical signals due to the pressure of a piezoelectric crystal by a seismic mass caused by the acceleration, while the load cells generate a variable current as the load cell can be subjected to strain or compression. The current signals arrive by micro-Lite 10-32 cables to the acquisition unit DIFA SCADA II where are converted in voltage, amplified and then sent to HP 715/100 unit.

The available signals can be processed in order to obtain all the information required about the vibrational phenomena occurring in the structure. On the workstation display it is possible to visualise in real time during the acquisition phase the applied force autospectrum, the multiple coherence of the various acceleration signals and the different frequency response functions both immediate and mediate. During the bonnet testing two electromagnetic shakers diagonally positioned, front (V455) and rear (V406), have been used. These shakers can generate a 196 N force (front) and 489 N force (rear) with air forced cooling.

Among the possible surrounding systems causing interference it can be considered a shaker vs. another. It has been necessary to avoid the creation of an energy transmission loop among first shaker-floor-second shaker-bonnet-first shaker. Practically it is necessary that the two shaking signals are not correlated each other.

The shaker connection to the tested structure presents some difficulties. It should be assured that shaking is applied in one axial direction and therefore the other 5 degrees of freedom should be disjointed. To allow it a steel push rod or stinger is used. In this way a high axial stiffness is obtained ensuring an optimal transmission of shaking force along the axial direction, while for the other directions the rod is flexible and therefore

able to buck only limited forces and resistant moments that could damage the shaker.

As far as the shaking signal a random one is chosen as it shakes at the same time all the modes in the concerned frequency field and can be fast as far as the acquisition time. Considering an average of signals the force spectrum is flat and continuos and contains energy almost constant on the whole concerned frequency field. The word random refers to shaking force amplitude and frequency.

To carry out the bonnet test, a random shaking signal has been used with a frequency range between 0 and 200 Hz.

The load cells have been positioned between stinger and structure. The connection with the structure is assured by a plate bonded to the bonnet with bi-component glue, having a threaded end on which the load cell is screwed. The load cell is equipped with a nut screw, while the stinger is secured by a cylinder with two threaded holes where on one side a stinger upper mandrel integral threaded rod is screwed and on the other side the load cell is screwed. To secure the accelerometers to the bonnet, Loctite glue has been used taking care to maintain the contact surfaces as much as possible clean in order to ensure a better frequency response.

The choice of response points is very important as it defines the validity of the subsequent validation and visualisation of the analysed structure modal shapes. Choosing few points, little time is required to acquire the FRF, but there could be spatial aliasing problems: it would be obtained a spatial resolution too low to be able to distinguish the different modal shapes. On the contrary by choosing many points a better resolution for the deformation visualisation would be obtained, but more time would be necessary to carry out the measurements. Moreover the response points should be positioned far from one or more structural modes, as on the contrary the measurement becomes difficult.

Finally the number, the positioning and the direction of shaking points are chosen as a function of the possibility of shaking at best all the resonances in the concerned frequency field. This has been made by the pre-test analysis.

Prior to carry out the FRF measurement in the points chosen on the structure it should be verified that the basis assumptions: linearity and reciprocity are met. Moreover also the quality of response functions in the guidance points should be good. To consider a system as linear it is necessary to verify that changing the force also the response changes in such a way the response/force ratio is constant. This means that the FRF of a perfectly linear structure should not depend from the shaking level. In the case analysed the bonnet has been subjected to two shaking levels, one the double of the other in a very sensitive point. From Fig. 9 it is possible to understand that the structure shows an enough linear behaviour in a high frequency range.

To meet the reciprocity assumption it is necessary to verify that the response of point i when applying the shaking at point j is equal to the response of point j when the shaking is applied at point i, i.e. it should occur that $(FRF)_{ij} = (FRF)_{ji}$.

Practically one shaker of the two has been alternatively connected to the structure. The first measurement has been carried out by positioning the shaker at point 3001 and the accelerometer at point 3002, the second measurement has been carried out by positioning the accelerometer at point 3001 and the shaker not connected before at point 3002.

Fig. 10 shows that the reciprocity assumption is met as the two frequency response functions coincide in a large frequency range. Moreover the resonance peak coincidence indicates that all the structural modes have been shaked.

The next phase, after the data acquisition, is FRF process. In practice from the acquired data are drawn those parameters, called modal that allow to re-create an analytical model that is the most similar (curve fitting) to the experimental one. To obtain these parameters there are different procedures having advantages and disadvantages, but all based on the same principle: the identification of the coefficients that join the measured data with the analytical ones.

Then it is possible to calculate some characteristical indexes that allow also an analytical verification. The most efficient evaluation method is the overlapping of FRF calculated on the measured ones: it is possible to directly judge the curve fitting made by the drawing method used. It is important to have a good coincidence in the resonance surrounds as the parameters calculated in their correspondence are representative of the whole system dynamic. At every frequency the structure dynamic behaviour can be characterised by their combination. Differences at one resonance (between synthetised and measured FRF) indicate a doubtful drawing at that frequency and for that degree of freedom. The possible causes of this discrepancy are the considerable presence of noise, the presence of unselected modes or a drawing method not suitable to the data, wrong approaches (e.g. analysed frequency intervals not ideal or frequency resolution not optimal for the data drawing in that defined interval).

The MAC or modal assurance criteria supplies a measure by an estimate at minimum squares of the dispersion of the different points representing the eigenvectors along the interpolation line. In this case it is defined as:

$$MAC(p,x) = \frac{\left(\{\Phi\}_p^T \{\Phi\}_x^*\right)^2}{\left(\{\Phi\}_p^T \{\Phi\}_p^*\right)\left(\{\Phi\}_x^T \{\Phi\}_x^*\right)}$$

and it is a scalar quantity, even if the mode is complex, ranging from 0 to 1.

If the modes coincide, it occurs that

$$MAC(p,x) = 1$$

while if the modes are linearly independent

$$MAC(p,x) = 0$$

For the low dumping structures, the estimated modal shapes should be normal with respect to the forcing, this means that the phase angle between two elements belonging to the same eigenvector could be 0°, 180° or −180°. An indicator called index of modal phase co-linearity (MPC) indicates the linear connection between the real part and the imaginary one of the eigenvectors. It should have a high value (about 100%) for the real modes. A low value indicates a complex mode due to local dumping in the analysed structure or to mistakes in the analysis procedure. Generally a MPC value <50% indicates the last cause. Another modal shape complexity indicator is the mean phase deviation (MPD), that represents the deviation with respect to their mean value and in-

dicates the modal shape phase dispersion. For the real modes this index should be very low (near to zero).

After having obtained all the FRF the modal parameters have been drawn. To calculate the frequencies and the modal dumping the Polyreference method has been used; then by LSFD the modal constants have been calculated (then the deformed ones) in order to take into account the lower and upper residual effects. A complex and then a real analysis have been carried out.

Table 3 shows the modal co-linearity and mean phase deviation index values for the complex analysis. It has to be noted that for the first ten frequencies the mode complexity is low. Moreover the values on Table 3 do not show any indication of mistakes in the analysis procedure

Modes	Frequency (Hz)	MPC (%)	MPD (°)	Phase dispersion	Mode type
1°	16.88	98.7	7.07	Low	Real
2°	18.14	86.9	28.29	High	Complex
3°	20.98	95.9	13.04	Low	Real
4°	22.12	99.0	6.26	Low	Real
5°	31.25	99.3	5.07	Low	Real
6°	37.13	98.6	6.99	Low	Real
7°	41.06	94.9	14.56	Low	Real
8°	51.31	97.6	9.49	Low	Real
9°	59.61	96.3	12.13	Low	Real
10°	63.08	87.0	24.10	High	Complex
11°	64.40	98.4	7.84	Low	Real
12°	68.74	95.3	13.59	Low	Real
13°	74.66	96.2	12.42	Low	Real
14°	83.80	83.3	26.60	High	Complex
15°	86.62	89.7	23.47	High	Complex
16°	90.24	80.5	31.59	High	Complex
17°	96.45	65.0	42.11	High	Complex
18°	97.26	75.5	36.18	High	Complex
19°	100.36	82.0	27.44	High	Complex
20°	103.95	95.6	13.36	Low	Real
21°	109.51	95.5	13.93	Low	Real
22°	112.96	89.4	20.85	High	Complex

23°	116.83	76.3	33.86	High	Complex
24°	118.61	85.1	25.14	High	Complex
25°	123.53	71.4	37.61	High	Complex
26°	126.58	77.8	34.28	High	Complex
27°	128.34	78.1	30.50	High	Complex
28°	132.15	43.7	56.09	High	Complex
29°	134.78	84.4	27.45	High	Complex

Table 3: Complexity index of the first 29

Table 4 shows the modal participation values, valuable both for complex and real analysis.

In the range from 0 to 200 Hz, 40 modes have been drawn of which the most important are the first 6 that range from 16.88 to 37.13 Hz (table 5), while the modes corresponding to higher frequencies are only higher bending shapes relatively less important.

The very low MAC values out of diagonal indicate a clear difference among the compared modes confirming a good drawing of modal parameters (Fig.11). The rare high value elements are representative of similar modes even if they occur at different frequencies; this means that a part of the deformation proceeds in the same way in the structure. It can be noted that raising in the frequency some modes tend to be similar when the index out of diagonal tends to increase.

modes	Frequency (Hz)	input:3001	Input:3002	TOTAL
1°	16.88	100.0	43.9	13.2
2°	18.14	52.6	100.0	3.1
3°	20.98	7.2	100.0	16.5
4°	22.12	100.0	57.4	12.0
5°	31.25	3.7	100.0	3.3
6°	37.13	58.6	100.0	3.8
7°	41.06	48.4	100.0	0.9
8°	51.31	100.0	59.5	1.1
9°	59.61	100.0	56.2	2.6
10°	63.08	100.0	10.1	1.8
11°	64.40	72.4	100.0	1.8
12°	68.74	100.0	23.3	2.6
ALL	//	48.9	51.1	100.0

Table 4 – Modal participation factors

Modes	frequency (Hz)	Type
1°	16.88	First bending plane xy
2°	18.14	Stiffening frame bending
3°	20.98	First torsional
4°	22.12	Second torsional
5°	31.25	Second bending plane zy
6°	37.13	First bending plane zx

Table 5: Frequencies and modes obtained in case of complex analysis

7.   Analytical/experimental model comparison

After having obtained both experimental and analytical results their comparison has been carried out. The main discrepancy causes among the results obtained in the two different types of approach can be resumed in the following causes:
- Assumptions made in the analytical mode; according to the type of elements which the structure has been discretized, different results can be obtained.
- Constraint problems; according to the constraint type both analytical and experimental, different results can be obtained.
- Slightly different analysed structure; in fact the analytical model derives from the structure drawing, while the experimental model is usually a workshop product always having some differences with respect to the model shown on the drawing, a slightly different behaviour could derive.
- Not coincidence of experimental measurement points with the analytical model nodes.

The index used to evaluate the analytical/experimental correlation is the MAC.

The mode comparison result is indicated by MAC index matrix shown on Fig. 12. The diagonal values lower than 0.7 indicate a non-optimal correlation as final result, but good as starting point for a next optimisation of the analytical model that can be obtained by suitable methods. [3,9]

In this case the MAC index is re-adapted as follows:

$$MAC(p,x) = \frac{\left(\{\Phi\}_p^T \{\Phi\}_x^*\right)^2}{\left(\{\Phi\}_p^T \{\Phi\}_p^*\right)\left(\{\Phi\}_x^T \{\Phi\}_x^*\right)}$$

where

$\{\Phi\}_p$ is the eigenvector of experimental modal shape components and $\{\Phi\}_x$ is the eigenvector of analytical modal shape components.

Experimental frequencies (Hz)	Analytical frequencies (Hz9	Difference %
16.88	17.313	2.56
18.14	19.202	5.85
20.98	21.405	2.02
22.12	23.171	4.75
31.25	33.112	5.96
37.13	37.991	2.32

Table 6: Frequency analytical/experimental comparison

8. Topological optimisation of the finite element model

The topological optimisation allows to define an optimal analytical model with respect to a chosen parameter that could be stiffness, volume or mass. Optimisation technique is based on two different approaches: numerical methods and optimum criteria. Numerical methods of optimisation are typically mathematical methodologies without physical information of the structure under study. Optimisation criteria come out from physical law that governing stress and strain distribution in the structure; when applicable, solution will converge faster.

For these last methods the physical and mechanical behaviour of the structure conduct to an optimum solution with, for example, stress minimisation and homogeneity. The bottleneck of these specific optimisation problems is the reduction of application to a limited area of the problem. An optimiser that uses such criteria is also a "controller" of the system itself because at every iteration the results are visible and it is possible to analyse them.

The use of optimum criteria requires new design rules, through "feedback optimum systems" : an analysis of sensitivity over design variables may be eliminated in this technique because the influence over full opimisation process is already outlined.

The controller function is as better as more precise is known the behaviour of the system. Optimisation criteria are divided into:

Shape Optimisation

The input parameters are the local node co-ordinates and the local node strains. The output parameters are the local modifications of the node co-ordinates the optimiser reduces the surface curvature by applying mass at points with high strains. For low strains the surface curvature is increased by removing mass at these points.

Topology Optimisation

The input parameters are the material distribution and the local element strains. The redesign rule tells how the required response has to be distributed regarding the boundary conditions and the set target mass so that the remaining mass will then be equally loaded considering all load cases. Starting from a homogeneous material distribution, mass will be compressed in areas of high energy density and diluted in areas of low energy density.

To simulate the dishomogeneous material distribution, the thickness of the shells versus Young's modulus are well suited; for solid structures using Young's modulus easily simulates the dishomogeneous material distribution.

Shape and topology controllers belong to "optimum criteria" optimisation group. They are based on the detection of an optimal contour of a component, in such a way to minimise the maximum stress. The objective is to minimise the maximum stress changing an assigned shape in a determinate variation area, i.e. an area in which surface or volume may be allowed to vary partially or totally.

The formulation of the shape optimisation problem [6] is the following (Fig.13):

An area $V \in IR^q$ $(q = 2,3)$ with the edge δV is given, whereby V respect δV are defined

by the component with respect to its edge. The maximum load stress B_{max} resulting from a prescribed component load shall be minimised by an "optimum edge" between two given edge points A and B belong to the same contour ($A, B \in \delta V$). The optimum edge ($\Gamma \in \delta V$) is required lying within a specific variation area Γ^*($\Gamma \in \Gamma^*$) defined by design boundary conditions so that load stress maximum is minimised in V. The maximum load stress derives from one or more load cases.

Shall have to verify the following conditions:
1. The law of stress decay is in effect, i.e. as much stress is high in a cutting area as much it decays faster, proportionally to the distance of the high stress area.

2. There is a maximum load stress on the component load edge δV.

If the maximum load stress exists on the edge δV within the variation area Γ^*, then the following theses apply to load case:

Thesis 1
a. The load stress on the edge Γ between two given points A and B is minimal, if the load stress on the edge Γ is constant.
b. A constant load stress on the edge Γ exists, if the edge Γ between the limiting points A and B does not adjoin to the border of the variation area Γ^*.

Thesis 2
a. If the edge Γ adjoins to the border of the variation area, the load stress on the portion Γ_f between the transition points A' and B' is constant and the load stress on the edges Γ_{ga} ($A\ A'$) and Γ_{gb} ($B\ B'$) is smaller than on Γ_f.
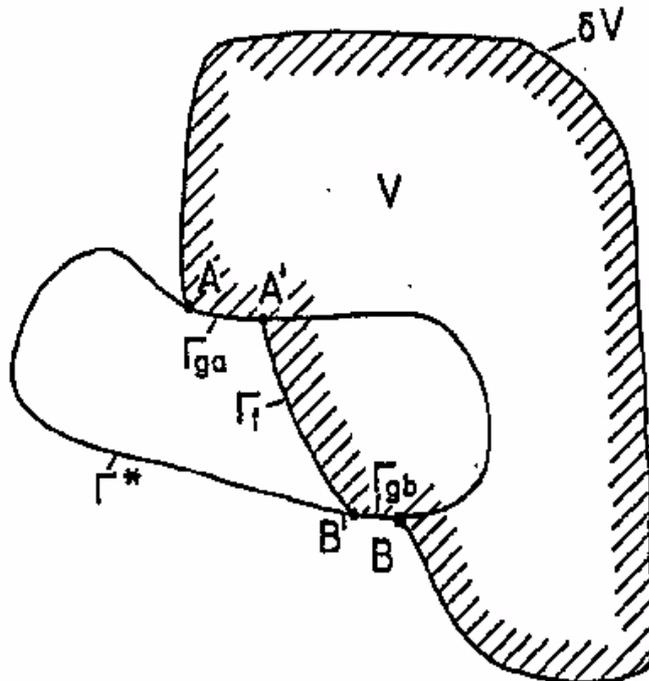
b. The longer the edge Γ_f is, the smaller the maximum load stress is on Γ_f. If Γ_f is equal to Γ, the load stress is minimal (if the variation limits A and B are

fixed).

For topological optimisation a basis project has to be used as start: a 2D or 3D area with homogeneous distribution of material, in which we want to operate has to be defined, in order to detect the optimum structural shape.

In this area the material distribution, at beginning homogeneous, becomes highly not homogeneous: zones without mass like holes and apertures together with high mass density areas will be created. The numerical difficulties will increase rapidly: the number of project variables typically ranges between 5000 and 100000. Topological optimisation maintains constant the model element number and does not change the nodal co-ordinates.

The Young modules E of the elements vary according to the stress and applied constraints. Modifying this module, an adjoin or removal of material is simulated: while "hard" elements have the same E of the beginner elements, Young module of the "soft" elements decrease in such a way to have no contribution to the stiffness of the structure. The size and dimension of the holes is so determined in a project space (2-D or 3-D) that at the beginning was filled with homogeneous distribution of material.

For the bonnet optimisation, the Topology module of the program MSC/CONSTRUCT based on the previous assumptions, has been used: it allows the topological structural optimisation of non-parametric models of mechanical stressed structures; peculiar characteristic is the reduction of weight in predesign phase. A static analysis with stress and strain results for the studied structure, before to execute the optimisation, is suggested with MSC/NASTRAN solution 101.

The Topology optimisation theory is based on the application of an energy equation to elastic systems. The energy equation tells that for elastic systems the outer work W_a is preserved without loss as shape change energy in the deformed system. According to the energy equation the shape change energy U yields from the identity with the external shape change energy W_a which results from the n applied generalised forces F_i to the structure

$$U = W_a = \frac{1}{2} \sum_{i=1}^{n} F_i \cdot w_i$$

For maximising the stiffness, the minimum of the strain energy has to be found.

During optimisation, the shape change energy U in the variation area is homogenised and minimised by specific changes of the compliance matrix. Introducing a fictive porosity the stiffness variation can be transformed into a density variation. Going in this way through massive computer use, simple but schematic results are obtained with solutions that never would be taken into account. For this, topological optimisation supplies freedom to engineer's creativity either in design phase or in manufacturing model master methods.

9.   Topological optimisation results

The optimisation results of the bonnet frame are now presented after the numerical validation of fem model to static and modal conditions.
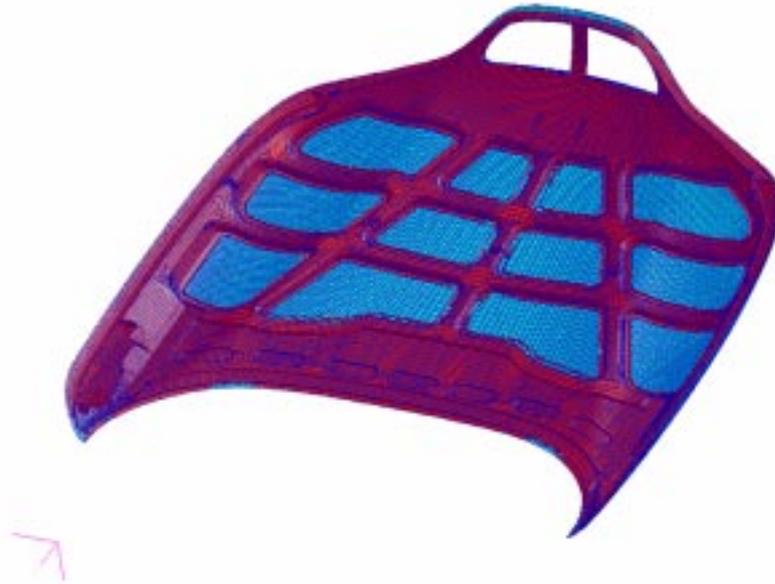

Figure 14: Start Configuration with design elements (red)

MSC/CONSTRUCT Topology has produced a valid support in optimising a predefined area of the bonnet in which pedestrian crash problems seems to be relevant at the moment of the re-design of the frame bonnet.

The optimisation results gives remarkable information about the distribution of the material in the frame in order to gain mass versus a little increase in z displacements and consequently reduction in torsional stiffness. Important instructions for the new Cad design frame are obtained and optimum energy distribution is pointed out.

The bonnet frame optimisation, Fig.14, has been done over 14 iterations. Starting from initial configuration, the third, eighth and fourteenth iteration cycles are visualised in Fig.15: a big decrease of volume is already visible since third iteration. Displacements and volume variations are represented in Fig.16.

On Tab.8 is reported the z displacement behaviour in mm after optimisation of the frame. Following a decrease of volume of 34.3% an increase of displacements is of 14.1% and the torsional stiffness achieves a final value of 28.24 N/mm for a torsion angle of 6.00 mrad. The weight reduction is about 3 Kg. Fig. 17 shows the new bonnet frame

Figure 15: Result of the Topology Optimization

design optimised to bending and torsional stiffness.

	Non optimised bonnet	Optimised bonnet	Variation %
Max Displacement (mm)	3.04	3.54	14.1
Torsional Stiffness (N/mm)	32.89	28.24	14.1
Volume (%)	100	65.7	34.3

Table 8: Variation of static variables following optimisation

For modal response point of view, the results are reported on Tab.9: a decrease of first bending frequency, due to elimination of material in a wide centre area, is obtained as expected, while torsional dynamic behaviour is improved for the good ratio between mass decrease and stiffness decrease.

Analytical frequencies for non optimised bonnet (Hz)	Analytical frequencies for optimised bonnet (Hz)	Modal shape	Variation %
17.313	15.814	1° bending	-8.65
21.405	22.512	1° torsion	+4.92

Table 9: Comparison between eigenfrequencies after optimisation

10. Conclusions

While shape optimisation will be better appreciated when fully integrated in CAD process, topology optimisation of MSC/CONSTRUCT is a powerful tool of design and seems to produce good results either in predesign phase and also when we have to act in some phases of the manufacturing process. Through the definition of non conventional shape for structure frame, true also for other IPF studied car components, the results obtained show a great decrease of weight with very little decrease of static performance with remarkable cost reduction.

The integration of a connected modal optimisation will be a powerful tool that will allow to close the design process of a car component, as outlined in this paper, with positive increase of all structural performance.
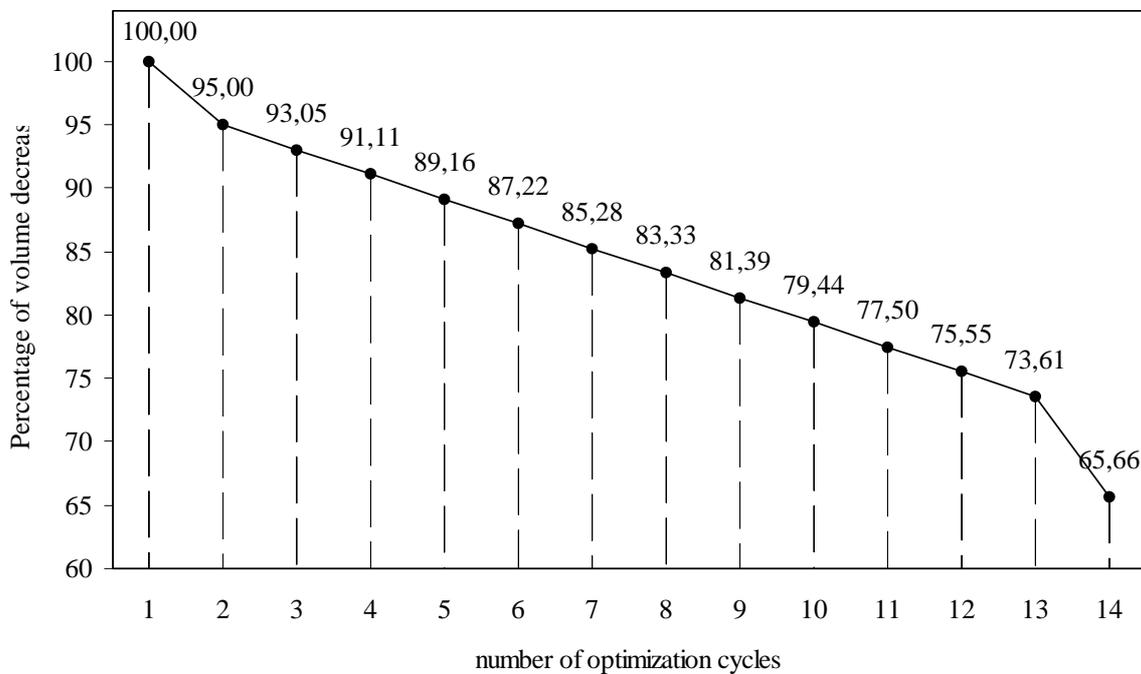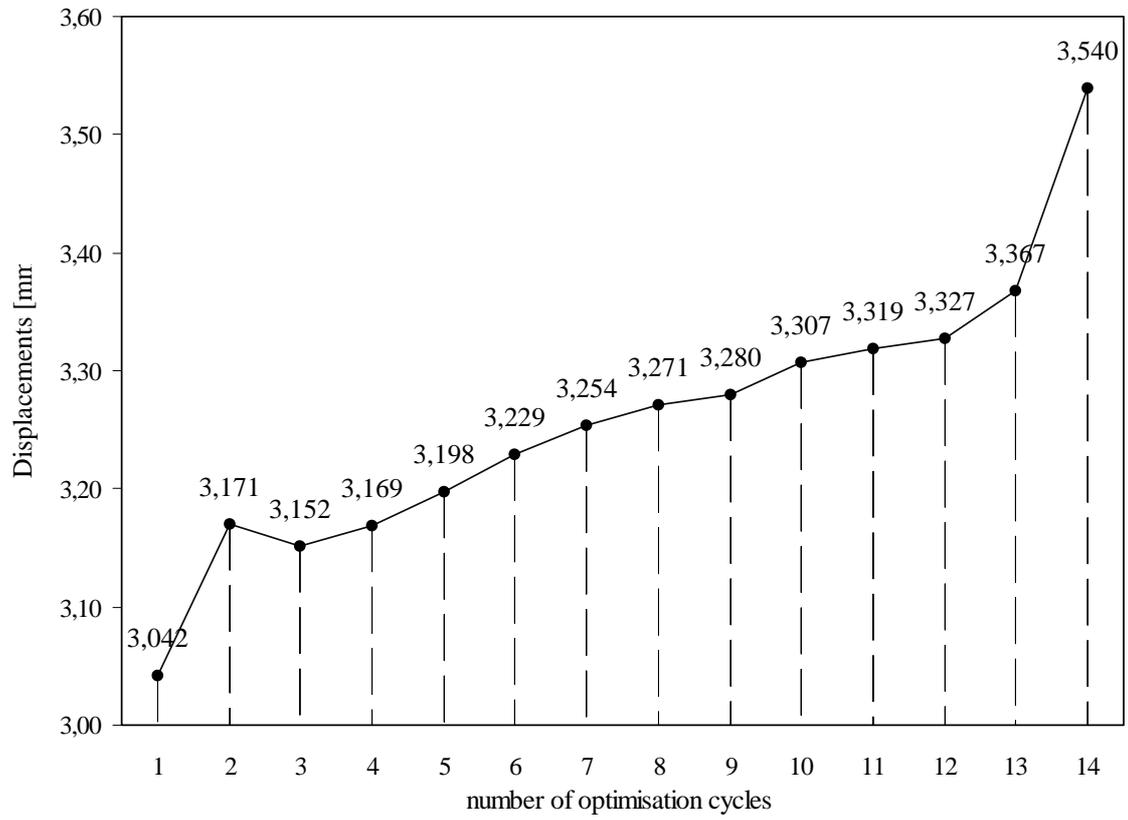
Figure 16: Displacement increase and percentage decrease of volume versus optimisation iterations.

11. References

[1]   M. Brugham, J. Leuridan, K Blauwkamp: "The application of FEM-EMA correlation and validation techniques on a body-in-white", L.M.S. Interleuvenlaan 65, B-3030 Heverlee, Belgium

[2]   D.J. Ewins: Modal testing: theory and practice, New York, John Wiley & Sons, 1984

[3]   N.A.J. Lieven, D.J. Ewins: "Spatial correlation of modes shapes, the Coordinate Modal Assurance Criterion", Dept. Of Mechanical Engin., Imperial College of Science and Technology, London

[4]   L.M.S Italia: "Corso pratico di analisi modale sperimentale", Novara 1994

[5]   LMS Users Manual: "Theory", L.M.S. Belgium

[6]   Allinger, Friedrich, Muller,Mulfinger,Puchinger,Sauter: Shape and Topology Optimisation using Caoss and MSC/Nastran, MSC World Users Conference, Universal City, 1995

[7]   MSC/CONSTRUCT: "Theory" User's manual, MacNeal-Schwendler Corporation, 1997

[8]   M. Vinci: "Progettazione statico-vibrazionale di un cofano con ottimizzazione topologica statica dell'ossatura e rielaborazione modale", Tesi di Laurea – Politecnico di Torino – Ingegneria Meccanica anno 1998

[9]   B. Piombo F. Furini G. Samele: "Analisi modale sperimentale MIMO di una scocca in alluminio e ottimizzazione del modello analitico a elementi finiti", MSC European User Conference, Roma, 1995